Laser-Induced Breakdown Spectroscopy Optimization of Tropical Hardwoods

by

Wesley Carson

A thesis submitted to the Faculty of the University of Delaware in partial fulfillment of the requirements for the degree of Degree in Chemistry with Distinction

Spring 2024

Laser-Induced Breakdown Spectroscopy Optimization of Tropical Hardwoods

by

Wesley Carson

Approved: Karl Booksh

Karl S. Booksh, Ph.D.

Professor in charge of thesis on behalf of the Advisory Committee

Approved: George W. Luther, III

George W. Luther, Ph.D.

Committee member from the Department of Chemistry & Biochemistry

Approved: Matthew F. DeCamp

Matthew F. DeCamp, Ph.D.

Committee member from the Board of Senior Thesis Readers

Approved: _____

Dana Veron, Ph.D.

Chair of the University Committee on Student and Faculty Honors

ACKNOWLEDGMENTS

I want acknowledge all of the professors within the department of chemistry & biochemistry who have provided me the knowledge and skills necessary to become a full-fledged chemist. In the laboratory itself, I want to thank Karl Booksh and Caelin Celani for the endless career and emotional support in guiding what has become my career as a chemometrician.

I also want to acknowledge Ellen Yurek for her guidance through Mentor Collective. Meeting weekly to discuss and revise both the thesis and my graduate school applications has undoubtedly been a strong factor in my undergraduate success.

TABLE OF CONTENTS

LIST OF TABLES

LIST OF FIGURES

ABSTRACT

Handheld laser-induced breakdown spectroscopy (LIBS) is being implemented to conveniently and effectively distinguish between various tropical hardwoods, a step toward combating illegal timber trade at ports of entry. A key parameter for LIBS analysis is the delay time between the laser pulse and spectral collection. Short delays yield more information-rich spectra with high noise while longer delays sacrifice information for a more stable spectrum. Currently, LIBS handheld spectrometers are designed for alloy and mineral classification, so the acquisition settings for the non-traditional - tropical hardwood – analysis should be re-optimized.

A subset of 23 species of hardwood were analyzed using various delay inputs, a collection parameter that dictates when sample plasma is analyzed by the instrument's detectors. The factory default setting for the LIBS handheld is 650 nanoseconds. Optimizing for these organic samples shows that a delay time between 250 and 370 nanoseconds yields a significant improvement in multivariate analysis of the collected spectra as evidenced in the increased accuracy of classification models. This improvement is demonstrated on a set of 280 exotic hardwood exemplars. This is meaningful for agencies such as the US Forestry Service (USFS) because it advises that imported hardwoods can be successfully identified in the field by handheld instrumentation such as LIBS.

Chapter 1

INTRODUCTION

1.1 Tropical Hardwoods

Tropical hardwoods are species of dense, slow-growing trees that originate in countries outside of the United States and, in many cases, are considered endangered. Species of hardwood, such as rosewood and cocobolo of the genus *Dalbergia*, are victims of illegal logging, an activity that comprises up to 30% of the hardwood traded internationally – a market that creates between 50 and 150 billion USD annually.[5] These woods vary greatly in grain pattern, coloration, texture, and other features that make them valuable as both decorative and artisanal materials.[2-4,7] Given the wide array of uses for these woods, countries that are typically rich with hardwood forests become a breeding ground for corruption and unregulated international trade.

The US has been facing increased challenges to keep illegally imported, endangered species of *Dalbergia* and related woods from making their way into the country through ports of entry. There are 275 species of *Dalbergia*, all of which are on the Convention of International Trade in Endangered Species (CITES) list as either endangered or at thread of becoming endangered.[5] Being on this list indicates that a given species of plant or animal is under threat of extinction. International trade of any specimen on the CITES list must be authorized via a licensing system. Despite the strict policies regarding import and export of endangered species, possible law enforcement isn't a strong enough deterrent to prevent illegal trade. In fact, the illegal

timber trade is a thriving market that has produced between 30 and 100 billion US dollars.[12]

Figure 1. 5 distinct species of tropical hardwoods used in the experiment

A defining trait of hardwood trees is the link between local soil chemistry and trace element uptake. Trace minerals contained in wood are directly linked with the soil in which the tree is grown, which is quite valuable given that species of *Dalbergia* are strongly correlated with location of origin. In other words, a crucial piece of information in understanding and mitigating the illegal timber trade is to relate intrinsic, trace elemental properties of a species of hardwood with its country of origin. By evaluating trace minerals within wood, narrowing down a sample of wood's provenance becomes an easier objective.

Typically, any discrepancy between reported wood identification and appearance would warrant a thorough investigation. In this case, a wood expert may identify a given piece of timber based on coloration, grain pattern, bark, density, and other morphologic traits; however, these considerations are typically subjective and not always immutable. Keeping an expert at ports of entry isn't always possible, which results in laboratory methods being another viable option. Laboratory-based methods are very reliable, but they tend to be both costly and time consuming, making them greatly inefficient.

One laboratory method of analysis, for example, Raman spectroscopy, has been found to accurately classify species of tropical hardwoods based on vibrational information contained within species of wood.[14] In several studies, near-infrared spectroscopy (NIRS) has successfully and accurately analyzed wood samples: one study successfully distinguished several Korean softwoods while another separated heartwood from sapwood.[10,19] Furthermore, x-ray fluorescence (XRF) has been implemented to determine elemental composition of wood waste products such as furniture wood, packaging material, and particle board.[7]

Although a laboratory analysis is a reliable and accurate method to validate the identity of incoming supplies of wood, the high volume of imports across the country necessitates both an efficient and real-time method for species identification – a new generation of handheld, field-portable chemical analyzers may solve this problem. The United States Forestry Service (USFS) in particular has funded the laboratory to critically evaluate handheld spectroscopy as a viable real-time method of analysis in tracing species of hardwood.

1.2 LIBS Spectroscopy

Laser-induced breakdown spectroscopy (LIBS) is a relatively new form of atomic emission spectroscopy (AES) that non-destructively analyzes samples in real-time with minimal sample preparation.[16-18,25] These devices are manufactured for qualitative analysis of metal alloys and geological material such as minerals without any necessary pre-treatment.[3,4,8,11,18,24] Fundamentally, the spectrometer uses a neodymium-doped yttrium aluminum garnet (Nd: YAG) crystal to focus and expel a high-energy, pulsed laser that ablates a nanogram quantity of material from the surface of a sample. From this ablation, a plasma cloud of elements and ions forms.

Using a series of charge-coupled device (CCD) detectors, photons emitted from elements excited in the plasma are converted into electrical signal and output as a spectrum of optical emission lines associated with different elements and their oxidation states. Another component of the handheld spectrometer is the argon cannister; an argon flush is utilized by the handheld to push airborne matter - primarily

water vapor - away from the path of the laser; this is necessary because contaminants reduce plasma formation and muffle signal intensities.

This method of analysis has been proven to be useful in analyzing a variety of materials in a diverse array of fields. For example, LIBS has been used substantially in planetary exploration[23], industrial metallurgy[9,15,21], and in determining hazardous articles.[22] In addition, Raman spectroscopy combined with LIBS has been effective in both qualitatively assessing mineral species and distinguishing between ores of the same chemical composition.[26]

1.3 Delay Input

Like all instrumentation, LIBS spectrometers are operated using a series of input parameters. These acquisition settings act as adjustable controls to improve or maintain the quality of spectra that is collected by the handheld. Currently, standard acquisition settings are optimized for aforementioned metal alloys and geological materials, though experimenting may prove useful for species of hardwood.

The most vital acquisition settings include number of shots, number of locations, and delay time. The number of shots indicates the quantity of ablations to be made by the pulsed laser whereas the number of locations indicates how many areas on the surface of the sample these shots should be made. The total number of shots applied to the surface of the sample is the product of the both quantities for these two settings.

The most important acquisition setting, integration delay, dictates at which moment after an ablation the detectors of the handheld will open for photon detection. Characteristic intensities of the ions contained within the plasma are greatest at the time of ablation, as seen in Figure 2[1]; however, later delay inputs return spectra that contain less chemical variance.[21]

It stands to reason that collecting photon emissions at the end of the plasma formation will result in the most unique elemental and ionic signals, though the volatile nature of the ions within the fresh plasma will result in a large shot-to-shot variability. Inversely, setting the integration delay to collect emissions after the plasma has cooled down will result in less characteristic spectral features. Most of the ionic species within the plasma will have created molecular structures, resulting in weaker signal intensities and decreased shot-to-shot variability.

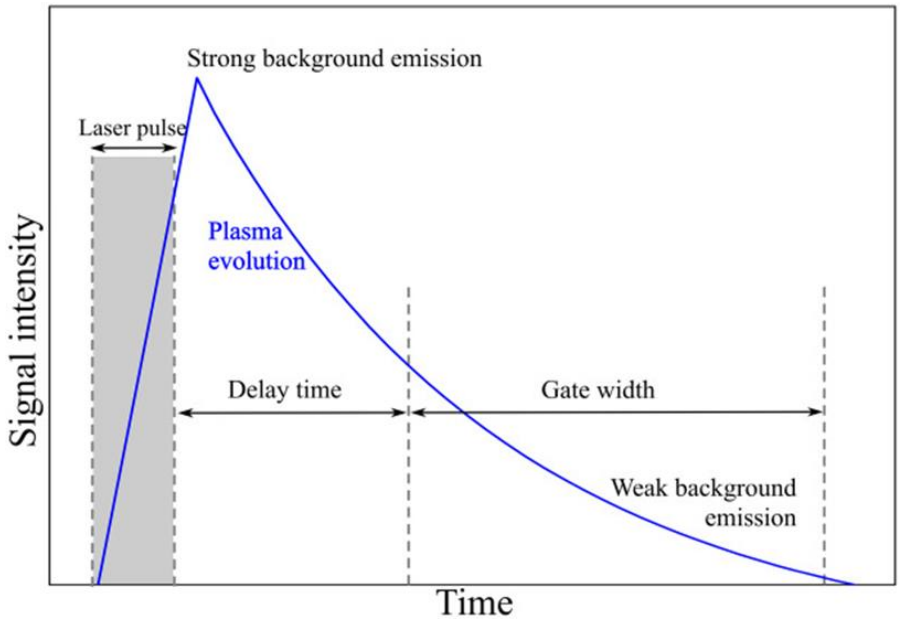

Figure 2. Signal intensity of plasma over time for sample LIBS[1]

1.4 Aims of the Study

The purpose of this study is to determine if the optimal delay input for timber – heterogenous, multivariate, organic material – differs from that of metal alloys – homogenous, univariate, inorganic material – and to adjust the analyzer's delay input setting, if so. To experimentally determine how unique chemical information contained within species of tropical hardwoods can most efficiently be extracted by implementing chemometric analyses. By analyzing data collected at various delay inputs with the chosen LIBS handheld, both the signal intensity and variance of the spectra obtained may be optimized for a more accurate hardwood classification and the optimal delay input setting can be numerically compared to the standard input value.

Chapter 2

METHODS AND MATERIALS

2.1 Full Set of Tropical Hardwood Samples

Wood samples of eleven *Dalbergia*, nine exotic hardwoods, and three species of unknown genus were obtained from the federal government, all of which are classified as heartwood – the dense, inner portion of a tree's cross-section. The non-*Dalbergia* samples were chosen based on provenance to assess if there is a correlation between *Dalbergia* and non-*Dalbergia* samples grown in similar locale. The wood chips were pre-cut in approximately 0.5 × 2 × 3 in. dimensions and had flat, smooth surfaces.

Table 1. Origins, class labels, and common name of wood samples

Class	Number of Wood Chips	Location	Genus Sp.	Common Name
1	12	Honduras	*Dalbergia stevensonii*	Rosewood
2	11	Madagascar	*Dalbergia spp.*	Rosewood
3	6	Brazil	*Dalbergia spruceana*	Rosewood
4	11	Surinam	*Dicorynia paraensis*	Angelique
5	16	Brazil	*Dalbergia cearensis*	Rosewood, Kingwood
6	13	Malaysia	*Dalbergia spp.*	Indonesian Rosewood
7	15	Brazil	*Dalbergia futascans*	Rosewood, Tulipwood
8	9	Mexico	*Dalbergia retusa*	Cocobolo
9	6	Madagascar	*Dalbergia maritima*	Rosewood
10	17	Tanzania	*Dalbergia Melanoxylon*	African Blackwood
11	8	Mexico	*Caesalpinia platyobe*	Chakte Viga
12	13	India	*Dalbergia latifolia*	Indian Rosewood
13	8	Mexico	*Caesalpinia enchinata*	Granadillo
14	17	Brazil	*Dalbergia nigra*	Brazilian Rosewood
15	13	Philippines	*Pterocarpus indicus*	Narra
16	16	Africa	*Pterocarpus soyauxii*	Padauk
17	11	Bolivia	*Machaerium scleroxylon*	Pau Ferro
18	14	Brazil	*Phoebe porosa*	Imbuia
19	14	Latin America	*Swartzia tomentosa*	Brazilian Ebony
20	5	Laos	*Pterocarpus indicus*	Amboyna, burl
21	7	Laos	Unknown	Flamewood
22	20	Laos	Unknown	Flamewood
23	18	Caribbean	Unknown	Mahogany

2.2 Instrumentation

In this analysis, a Sci-aps Z-300 LIBS handheld instrument was used, as seen in Fig. 2. Device specifications, such as the excitation source, include a 1064 nanometer, 5 millijoule pulsed laser that has a repetition rate as fast as 50 Hz. Contained in the handle of the device is a replaceable argon cartridge necessary for an argon purge environment, usable for approximately 600 scans.

The handheld operates using an Android touch-screen interface that implements an on-board camera for sample viewing before, during, and after the surface ablation. A focusing feature allows the position of the laser to be automatically applied and manually adjusted. Data collected is stored on the 8 Gigabyte internal SD.

These device specifications make the Z-300 model a suitable method of analysis given the large quantity of spectra that can be stored, the ability to view the surface of the sample as it is being analyzed, and the powerful laser source that is emitted.

Figure 3. A Sci-aps Z-300 LIBS handheld spectrometer.

2.3 Acquisition Settings

There are several acquisition settings of the LIBS spectrometer that are fundamental to how it performs, as seen in Table 2. For example, number of locations and number of shots determine the number of spots on the sample's surface to ablate

with the pulsed laser, as well as the number of shots per location, respectively. Cleaning shots per location indicates the number of burns applied to each location across the surface of the sample; this serves to clean the sample's surface of any residual debris and contaminants.

Integration times are the most important in determining spectra quality. The integration period, often known as the gate window, dictates how long the CCD detectors will analyze photon emissions; longer integration periods will improve a spectrum's signal-to-noise ratio and smooth the spectral curve. For this experiment, the integration time was set to a numerical input of 0, which indicates a time of a few microseconds. Per conversations with the manufacturer, Sci-aps, adjusting the integration time is futile because the setting control isn't sensitive enough to meaningfully sample the plasma and, therefore, spectral output. The integration delay determines the time at which the device's CCD detectors begin collecting optical emission signals following the laser pulse. For materials such as metal alloys, Sci-aps sets the factory delay time to a numeric input value of 19 – this translates to 650 nanoseconds.

Table 2 Example Acquisition Settings of Sci-aps Z-300 LIBS handheld spectrometer used in validation data collection.

Setting	Input
Number of Locations	8
Cleaning Shots per Location	2
Data Shots per Location	8
Step Size	24
Integration Period	0
Integration Delay	19
Argon Flush	300
Start Location	204, 126, 60
End Location	276, 174
Reset Stage	Yes
Use Gating	Yes
Test Rate	10 Hz
Clean Rate	10 Hz
Linear	Yes
Random	No
Avg. Spectra	No
Shots to Avg.	N/A

2.4 Experimental Design - Optimization

For the rough optimization, delay inputs ranging from the lowest delay time allowed to just under twice the factory setting were implemented. These values are 250, 376, 502, 650, 817, and 985 nanoseconds. The handheld analyzer however, requires integer instrumental settings with a numeric input of 0 corresponding to 250 nanoseconds and 19, as previously mentioned, corresponding to 650 nanoseconds. Thus, each incremental setting is, approximately, a 21 nanosecond increase.

Four classes were randomly selected for the preliminary screening of delay times with the constraint that all classes chosen must have at least 8 unique timber samples. Consequently, 32 wood samples spanning 4 classes were analyzed to determine the best range of delay times to use for timber classification models.

Each sample of wood was scanned 6 times. The pulse laser was set to shoot onto 8 separate locations at a rate of 12 ablations per location. At each location within a single scan, the 12 ablations were averaged into a single spectrum, and all 8 locations were averaged into a single overall spectrum. Across 4 classes, 8 samples per class, and 6 average spectra per sample, a total of 192 spectra were output during the initial optimization.

Table 3. Hardwood sample quantity and species information from initial optimization.

Class	Number of Wood Chips	Location	Genus Sp.	Common Name
1	8	Honduras	*Dalbergia stevensonii*	Rosewood
5	8	Brazil	*Dalbergia cearensis*	Rosewood, Kingwood
7	8	Brazil	*Dalbergia futascans*	Rosewood, Tulipwood
19	8	Latin America	*Swartzia tomentosa*	Brazilian Ebony

Following the results of the initial optimization, delay inputs 0, 2, 3, 4, 10, and 19 were used for the secondary analysis. These delay inputs spanned 250 to approximately 335 nanoseconds, with 460 and 650 nanosecond values included as

reference to the initial optimization. In regards to class, 4 of the 16 classes that contained 10 or more samples were randomly chosen, as shown in Table 3. Because we were looking for a more subtle effect, there was a priority on reducing intra-species variance; therefore, the quantity of samples per class was increased from 8 to 10. 10 samples from each of those 4 classes were randomly chosen, resulting in a sample population of 40 wood samples.

The acquisition settings remained the same as for the prior analyses except for the number of shots applied to each location on the surface of a sample: this was changed from 12 to 8 shots. The average of the 8 shots were used to build classification models.

Table 4. Number of samples and species from second optimization.

Class	Number of Wood Chips	Location	Genus Sp.	Common Name
5	10	Brazil	*Dalbergia cearensis*	Rosewood, Kingwood
7	10	Brazil	*Dalbergia futascans*	Rosewood, Tulipwood
10	10	Tanzania	*Dalbergia Melanoxylon*	African Blackwood
22	10	Laos	Unknown	Flamewood

2.5 Experimental Design – Validation

Following the results of the optimization, two complete sets of data were collected to compare and validate the chosen optimized delay input to that of the

standard, factory setting. Both the chosen optimized delay input and the standard setting, instrument setting values two and nineteen, were implemented in collecting data on all 278 available wood samples. Acquisition settings employed during the fine optimization were re-used; 8 shot locations and 8 data shots per location following 2 cleaning shots, resulting in a total of 64 shots that would be averaged into a single spectrum for every scan.

Unlike the most recent optimization, however, both the quantity of scans and scan location have changed. The number of scans for any given sample increased from 5 to 13. 10 of these 13 scans were radial scans, as they were applied to the flat region of the sample, orthogonal to the grain. The other 3 were axial scans, shots applied directly into the grain.

2.6 Software

Sci-aps Profile Builder program version 2.19.1a, which comes bundled with the handheld instrument, was used to display, label, and export all collected spectra as comma separated values (CSV) files. In addition, R programming language and Rstudio integrated development environment (IDE) were used for all data processing and analyses. This experiment used R version 4.3.1 and Rstudio version 2023.06.0+421.

2.7 Data Importation

Data are imported into R using the base function “read.csv.” Each CSV file is imported and subsequently placed as a row in a raw data matrix; the number of rows reflects the quantity of spectra and the number of columns indicates the quantity of wavelengths analyzed by the LIBS handheld analyzer.

2.8 Pre-processing Methods

A raw LIBS spectrum must be processed in multiple forms before it can be properly analyzed. Spectra from the LIBS handheld contain leading and trailing zeros, wavelengths which collected no spectral information, so these values are truncated across all samples; this is approximately 600 variables, dropping an output of 23,431 wavelength values down to 22,850.

The LIBS handheld utilizes three CCD cameras to detect photon emissions in different wavelength ranges. There are two noticeable ‘jumps’ in every spectrum; each jump indicates a switch from one detector to the next. To adjust the spectra such that each section is positioned equally, an Asymmetric Least Squares (ALS) filter, sourced from the ‘baseline’ package in R,[6] was fit on each of the three sections of data. The benefit of utilizing this particular method of baseline correction is that it optimizes and validates the model of best fit in favor of applying a pre-defined mathematical function. After applying the ALS filter to each of the three sections of the raw output, they were concatenated back into a single spectrum.

Following baseline correction, each sample was normalized to unit area. This removes sample-to-sample variance that may result from differences in data collection

based on how the sample is placed upon the analyzer prior to each scan. Figure 4 represents a baseline correct and normalized plot of a all spectra collected at a delay time of 250 nanoseconds. Figures 5 and 6 show baseline fit and normalized spectra of three species – two *Dalbergia* and one unknown – at two series of wavelengths in which they all clearly distinguish from one another.

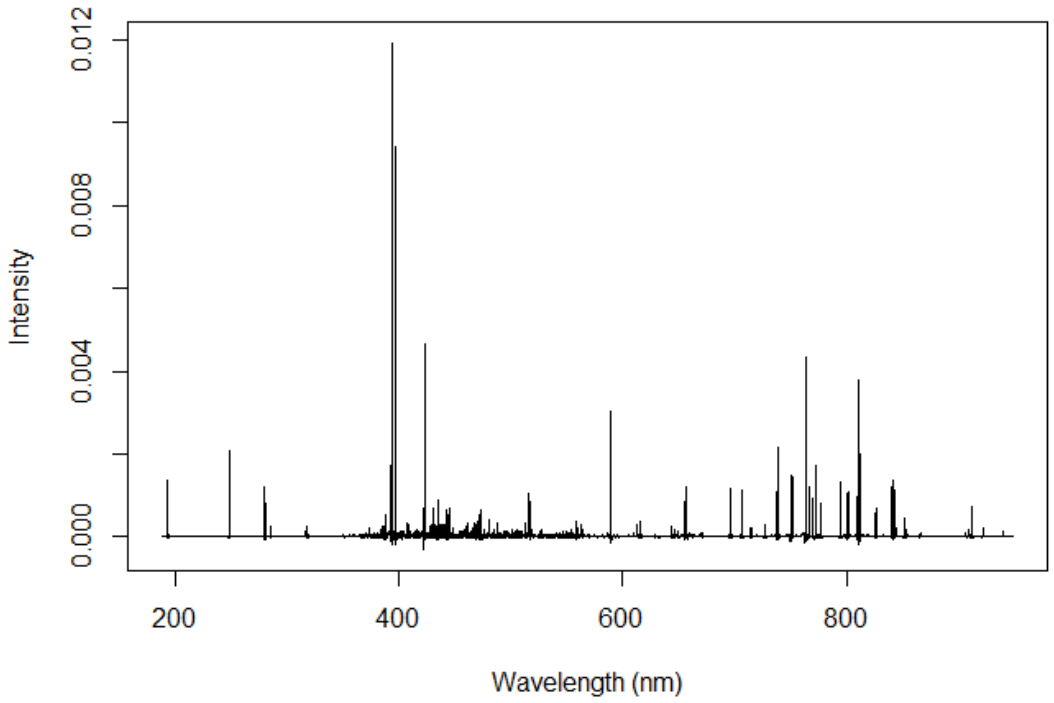

Figure 4. Plot of data that was collected at a delay input of 250 nanoseconds. The matrix columns were baseline fit, normalized, and averaged.

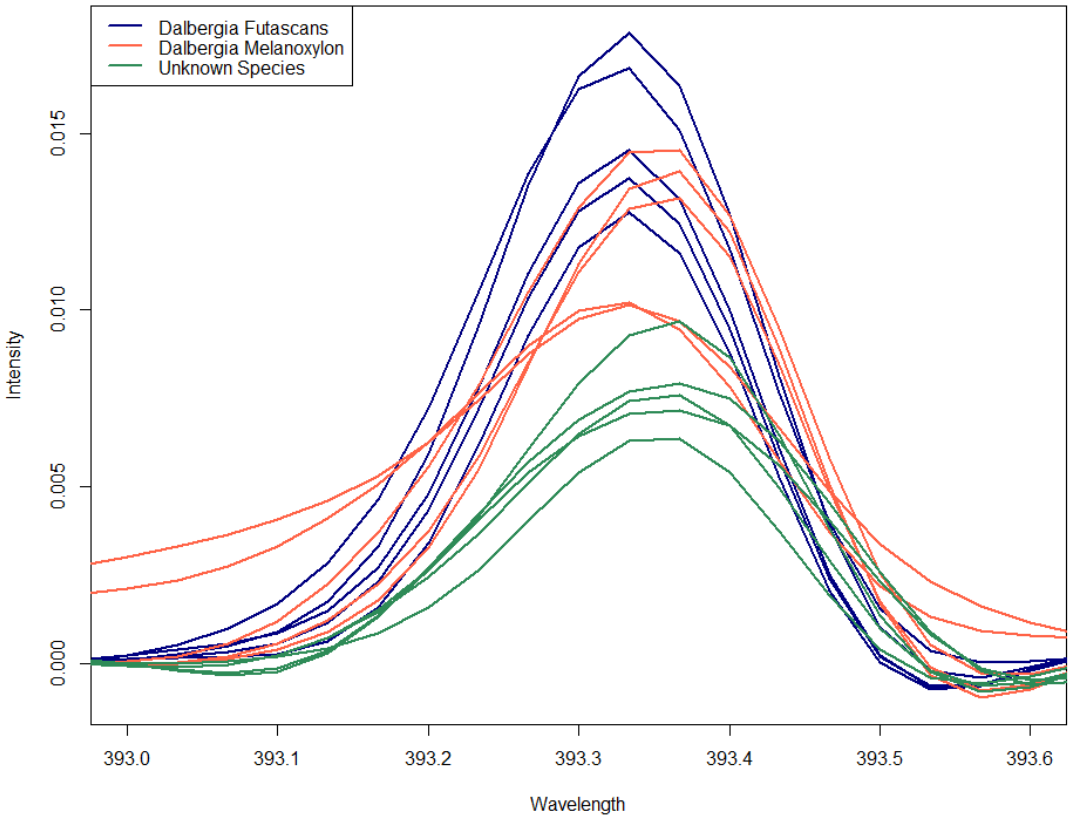

Figure 5. Baseline corrected, normalized spectra consisting of three species. Wavelength ranges from 393 to 394 nanometers.

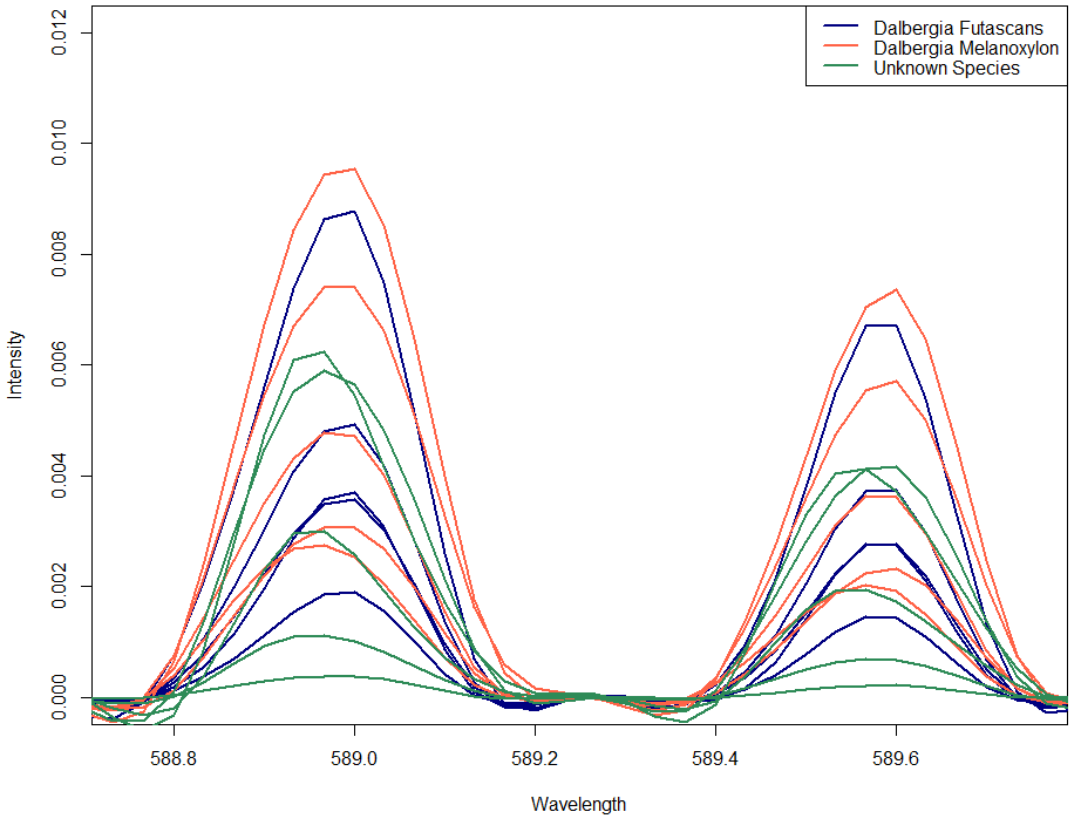

Figure 6. Baseline corrected, normalized spectra consisting of three species. Wavelength ranges from 588 to 590 nanometers.

Next, a form of variable selection was implemented to reduce each spectrum's overall signal-to-noise ratio. By hand-selecting the peaks that contain meaningful chemical information, model efficacy is improved and undesirable information is minimized. Regions that contained no chemical information – for example, baselines – or were related to the handheld's argon purge were removed.

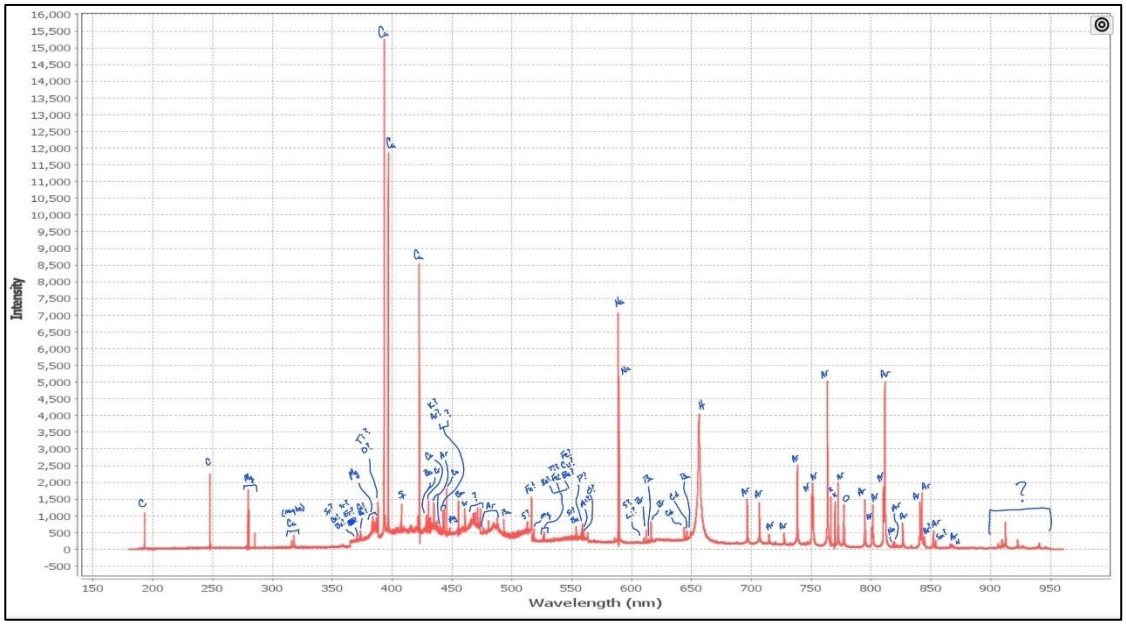

Figure 7. LIBS spectrum of hardwood sample in Profile Builder software. Peaks are labeled with identifying elements.

2.9 Modeling Methods

In this work we employed 1-vs-world models, as well as flat classifiers. In a flat classification, models best separate all classes from one another. This method of analysis is particularly useful in determining how well the data associated with a given class overlaps with other classes. As a result, misclassifications between classes of similar span of data can be visualized using network plots.

In a 1-vs-world classification, there is a single class of interest, and everything outside of it is granted a new class identification. In contrast to a flat classification, this method evaluates how well a single class can distinguish itself from the rest of the data when the decision outcome is binary.

Two particular modeling methods within the classification and regression training (CARET) package in R were used to analyze the pre-processed data: support vector machines discriminant analysis (SVM-DA) and partial-least squares discriminant analysis (PLS-DA). These machine-learning algorithms capture and optimize the most identifying sets of information within a set of data and use that to create models that can be used to make predictions.

PLS-DA is a dimensionality-reduction method that utilizes class information for optimal class separation. This method maximizes the covariance between sample data and corresponding class values by calculating a linear subspace that encapsulates input sample information – this new space is made of potential variables, otherwise known as components. PLS-DA maximizes the variance contained at the first component onward such that, ideally, majority of the original sample space will be expressed in as few components as possible. Given this, the first several components can be expressed as a 2-D or 3-D plot to easily visualize class separation.

SVM-DA is another supervised machine learning method that maximizes separation of classes. This method uses a combination of mathematic variables to create an n-dimensional hyperplane – based on a sample space of n-variables – that maximizes the distance between two classes as a means to separate them. The support vectors are the data points that are closest to the hyperplane, the points that are most heavily used in calculating the decision boundary. A 2022 study found that SVM, among other techniques such as k-nearest neighbors (k-NN) and Neural Networks, are particularly useful in classifying various classes of wood.[13] There are numerous variations of SVM, such as linear, radial, and polynomial, to name a few; though, this study will focus solely on linear SVM-DA as a method of classification.

2.10 Cohen's Kappa and Accuracy Metrics

There are two useful metrics in determining how well a classification model performs: accuracy and kappa. Accuracy of a model is determined by the correct number of classifications made relative to the total number of samples. This metric is great for balanced applications, such as flat classifications, where the quantity of samples across classes are either equal or consistent. Where accuracy commonly falls short, however, is when evaluating the performance of a 1-vs-world model. In 1-vs-world models, it is common for the relatively small class of interest to misclassify entirely, while the larger, remaining set of data is perfectly predicted. The accuracy of such a model indicates that it performs almost impeccably, but this is clearly not the case.

Alternatively, Cohen's Kappa is a metric that evaluates the observed accuracy of a model while simultaneously accounting for the expected accuracy obtained by randomly guessing.

$$k = \frac{P_o - P_e}{1 - P_e}$$

P_o is the percentage of spectra that have been correctly predicted by a model, while P_e is the expected accuracy by simply guessing - a value that is always greater than zero. Much like the aforementioned accuracy metric, a perfect classification results in an output of 1. In the case of a 1-vs-world model, a kappa metric will provide a much more consistent evaluation of model efficacy than accuracy.

2.11 Cross-validation Optimization

Once a modeling method was chosen, cross-validation (CV) was implemented to optimize the robustness of the model. CV is a modeling control technique that splits a training set of data by some percentage and iterates through all possible combinations of adjustable model parameters to determine the best performing version of the model.

Used here is a particular variant of CV known as 'repeated K-folds CV.' The 'folds' determine the quantity of splits across the training set of data. For example, an input of 10 causes the training data to be randomly split into 10 uniform groups of data. The model is then created and validated 10 times; each time, 9 of the 10 groups are used to train the model and the remaining set's class information is predicted by the model. This is known as 'jackknifing.'

The process is repeated numerous times to better reflect the true estimation of expected model performance. The initial training data will again be uniformly split based into the desired number of folds with a new, random selection of data: this is referred to as 'bootstrapping.' By repeating a CV, overperformance of a model is minimized. The maximum cross-validation kappa of each fold in a single repeat is output and subsequently averaged with the values of the other repeats; this ensures that the model is not overfitting the data and is best utilizing the information being fed into it.

2.12 Confusion Matrices

Confusion matrices are a numerical method to visualize successes and failures of a classification model. Each sample in a set of data has a particular class value attached to it that correlates directly with what species of wood it originates. Each species of wood is also indicated by an integer value, spanning anywhere from 1 to 23. The true class values, known as the class vector, contain the correct, corresponding specie label for each sample and its spectra. After a classification model is performed on a set of validation data, a prediction vector, containing the same number of elements as the class vector, is obtained. These two vectors are paired and evaluated at each index to check if the model predicted each sample correctly and, if not, what class was the sample incorrectly identified as.

The collection of these class values within the class vector and the prediction values from the model's output can create an n-by-n, square matrix, as shown in Fig. 5. A perfect classification contains the total number of spectra from each class at its respective location along the diagonal of the square matrix. As an example, if all 'n' values contained within class 'x' of the validation set are accurately classified as class 'x,' then we'd expect a value of 'n' at the x-th spot along the diagonal of the confusion matrix. Values that are not contained along the diagonal, then, indicate a sample that has been incorrectly predicted as a separate class.

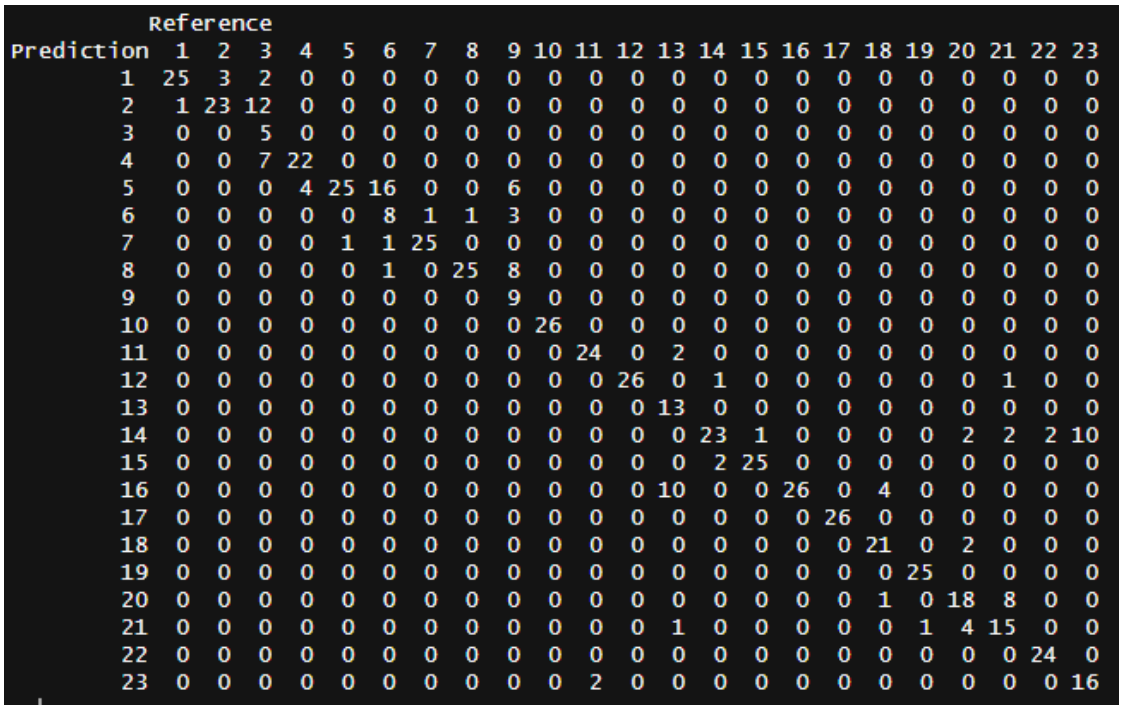

	Reference																						
Prediction	1	2	3	4	5	6	7	8	9	10	11	12	13	14	15	16	17	18	19	20	21	22	23
1	25	3	2	0	0	0	0	0	0	0	0	0	0	0	0	0	0	0	0	0	0	0	0
2	1	23	12	0	0	0	0	0	0	0	0	0	0	0	0	0	0	0	0	0	0	0	0
3	0	0	5	0	0	0	0	0	0	0	0	0	0	0	0	0	0	0	0	0	0	0	0
4	0	0	7	22	0	0	0	0	0	0	0	0	0	0	0	0	0	0	0	0	0	0	0
5	0	0	0	4	25	16	0	0	6	0	0	0	0	0	0	0	0	0	0	0	0	0	0
6	0	0	0	0	0	8	1	1	3	0	0	0	0	0	0	0	0	0	0	0	0	0	0
7	0	0	0	0	1	1	25	0	0	0	0	0	0	0	0	0	0	0	0	0	0	0	0
8	0	0	0	0	0	1	0	25	8	0	0	0	0	0	0	0	0	0	0	0	0	0	0
9	0	0	0	0	0	0	0	0	9	0	0	0	0	0	0	0	0	0	0	0	0	0	0
10	0	0	0	0	0	0	0	0	0	26	0	0	0	0	0	0	0	0	0	0	0	0	0
11	0	0	0	0	0	0	0	0	0	0	24	0	2	0	0	0	0	0	0	0	0	0	0
12	0	0	0	0	0	0	0	0	0	0	0	26	0	1	0	0	0	0	0	0	1	0	0
13	0	0	0	0	0	0	0	0	0	0	0	0	13	0	0	0	0	0	0	0	0	0	0
14	0	0	0	0	0	0	0	0	0	0	0	0	0	23	1	0	0	0	0	2	2	2	10
15	0	0	0	0	0	0	0	0	0	0	0	0	0	2	25	0	0	0	0	0	0	0	0
16	0	0	0	0	0	0	0	0	0	0	0	0	10	0	0	26	0	4	0	0	0	0	0
17	0	0	0	0	0	0	0	0	0	0	0	0	0	0	0	0	26	0	0	0	0	0	0
18	0	0	0	0	0	0	0	0	0	0	0	0	0	0	0	0	0	21	0	2	0	0	0
19	0	0	0	0	0	0	0	0	0	0	0	0	0	0	0	0	0	0	25	0	0	0	0
20	0	0	0	0	0	0	0	0	0	0	0	0	0	0	0	0	0	1	0	18	8	0	0
21	0	0	0	0	0	0	0	0	0	0	0	0	1	0	0	0	0	0	1	4	15	0	0
22	0	0	0	0	0	0	0	0	0	0	0	0	0	0	0	0	0	0	0	0	0	24	0
23	0	0	0	0	0	0	0	0	0	0	2	0	0	0	0	0	0	0	0	0	0	0	16

Figure 8. Example confusion matrix from full dataset collected at 650 nanoseconds, the factory delay setting.

Chapter 3

RESULTS

3.1 Analysis of the Rough Hardwood Optimization

The rough optimization maximizes the kappa metric across both models at values 250 and 950 nanoseconds. For the SVM model, Fig. 6 shows a general downward trend from an input of 250 nanoseconds down to 950, indicating an optimization value at an instrument input of integer value zero. The PLS model shown in Figure 7, similarly, shows a downward trend from 250 to 950 nanoseconds; however, the models indicate a maximum model efficacy at an instrument delay time input of zero – 250 nanoseconds.

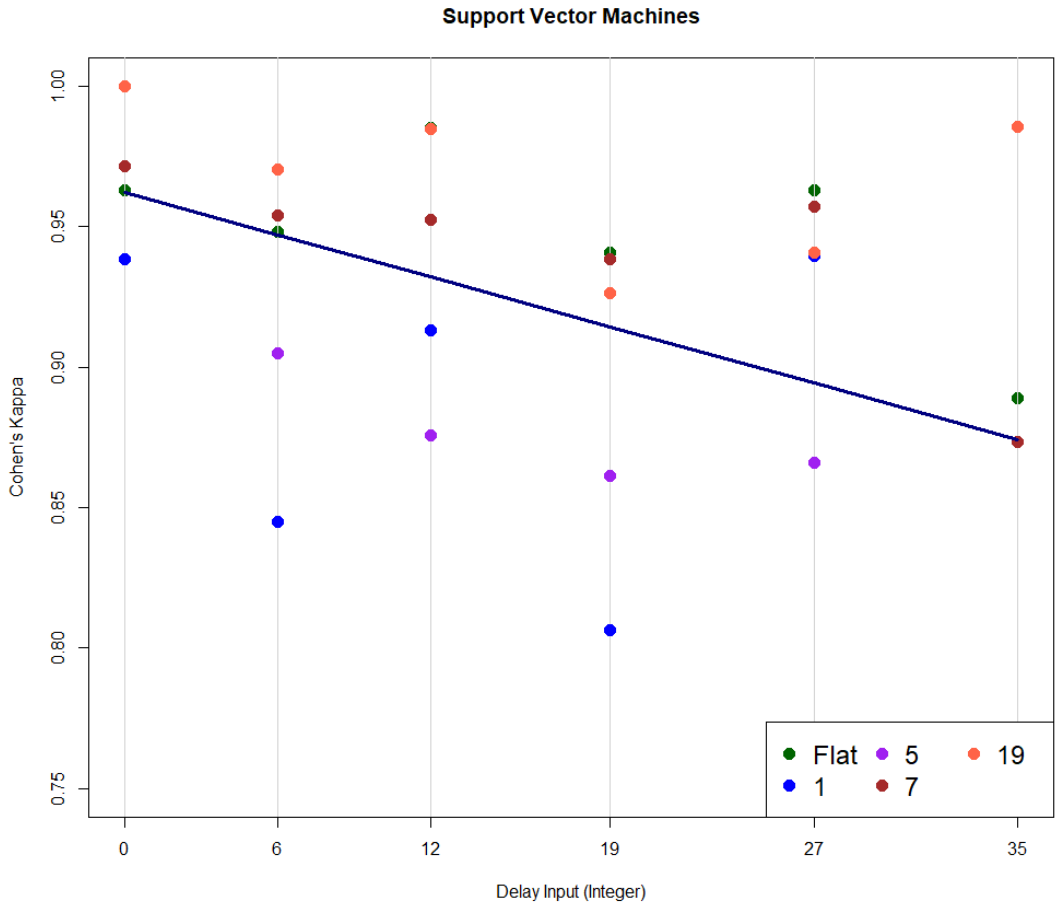

Figure 9. Plot of 1-vs-world kappa values from pre-processed data using an SVM model.

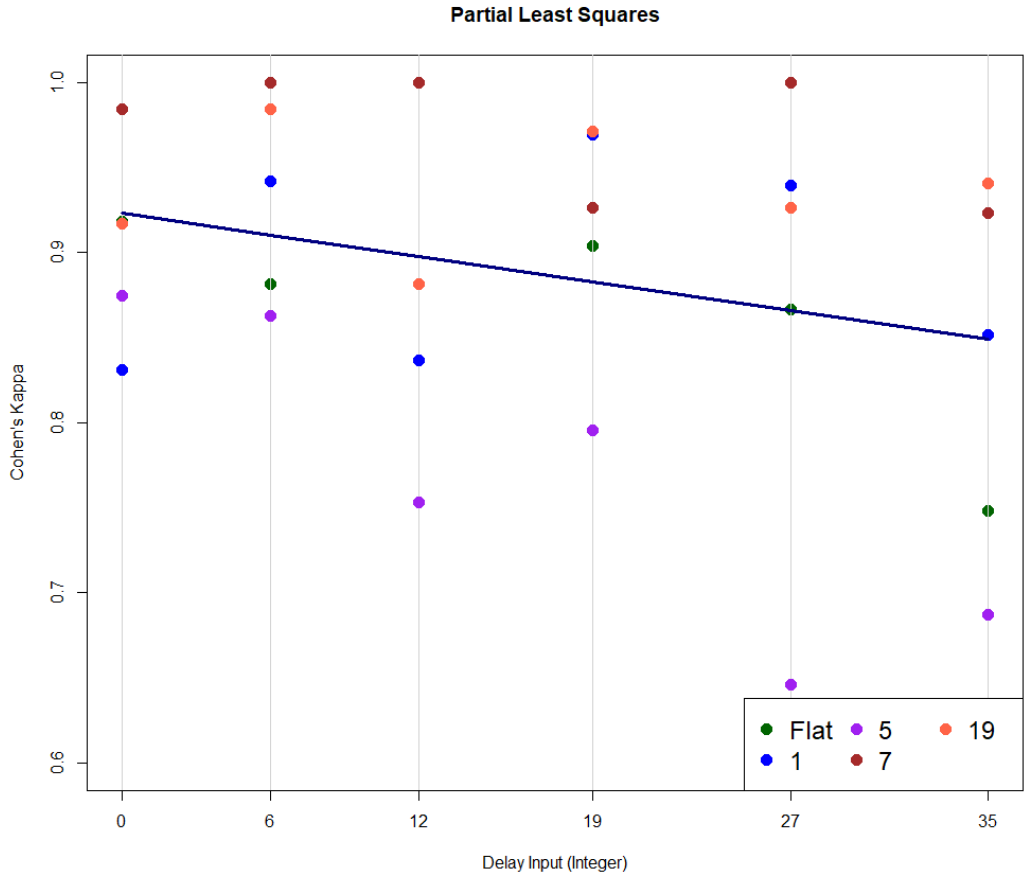

Figure 10. Plot of 1-vs-world kappa values from pre-processed data using a PLS model.

3.2 Analysis of the Fine Hardwood Optimization

The fine hardwood optimization doesn't have as clear results. In Fig. 8, a maximum SVM model performance was observed at delay input values 4 (330 ns) and 10 (450 ns), with the best performance in the range of 450 to 630 nanoseconds – the factory delay setting. Further, the PLS model shows a positive, increasing trend in performance across delay time, with a maximum output at the factory delay input.

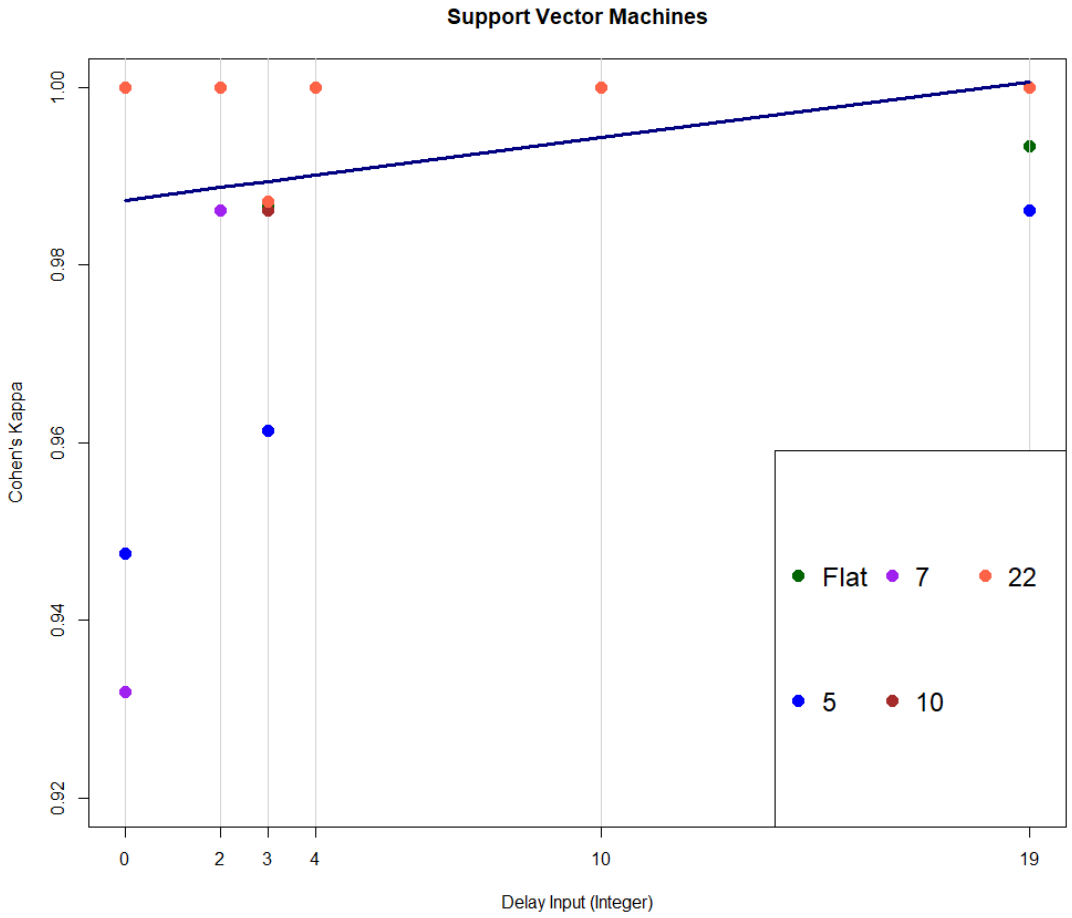

Figure 11. Plot 1-vs-world kappa values from pre-processed data using an SVM model.

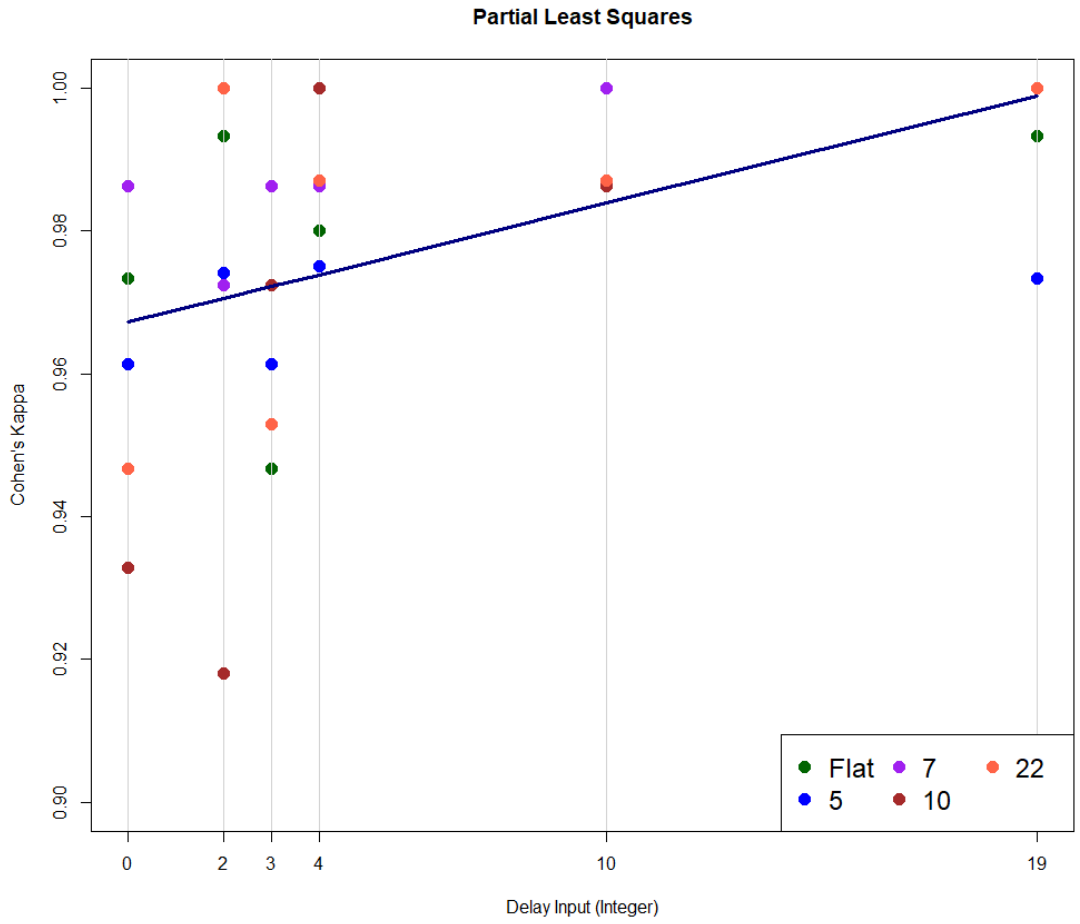

Figure 12. Plot of 1-vs-world kappa values from pre-processed data using a PLS model.

3.3 Analysis of Factory Standard Delay Against Optimized Delay Input using SVM Models

At the factory standard delay input, the flat classifier of all 23 species using an SVM model had an average prediction kappa of 0.797 with a standard deviation of 2.24×10^{-2} across 5 repeats. Boxplots are colored orange and outliers are denoted by downward-facing, purple triangles. The 1-vs-world analysis had an average prediction

kappa of 0.696 with a standard deviation of 3.06×10^{-2}, as indicated by the horizontal line in Figure 11.

Network plots, as shown in Fig. 10, provide a convenient way to visualize confusion matrices. Each class is represented by a navy-colored node, and misclassifications – the off-diagonal values in a confusion matrix – are indicated by a wine-colored arrow. The head of an arrow points in the direction of the misclassification such that an arrow pointing from class 16 to class 13 represents a sample from class 16 that was incorrectly predicted to be a member of class 13. The thicker the arrow edge, the greater quantity of misclassifications.

Figure 10 had 105 misclassifications across 21 of the 23 species of wood. Most misclassifications were in a single direction, as exemplified by 14 to 23, 12 to 14, and 11 to 13, to name a few. While most of the failed predictions occurred for only a few spectra, there are a few noticeable classes that had many misclassifications; 10 spectra from class 12 were incorrectly identified as class 21, and 8 from class 19 were misrepresented as class 21.

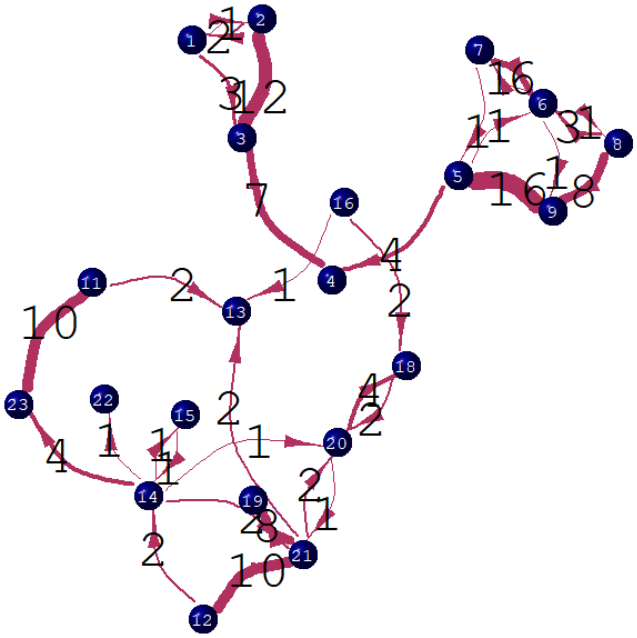

Figure 13. Network plot of the flat classifier confusion matrix at the factory setting delay time.

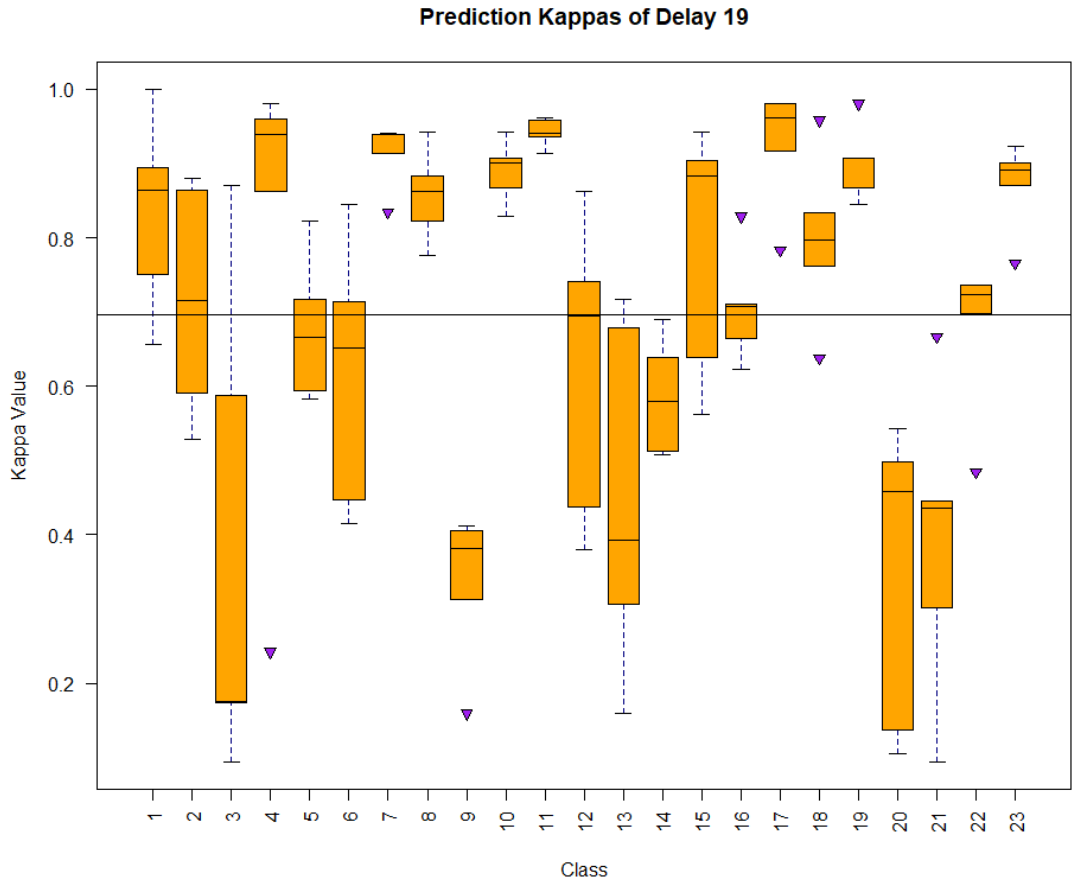

Figure 14. Boxplot of 1-vs-world classification at factory setting delay time.

At the chosen, optimized delay input, an input of 2, the flat classifier of all 23 species using an SVM model had an average prediction kappa of 0.900 with a standard deviation of 5.29×10^{-2} across 5 repeats. Shown in Figure 12, 13 misclassifications occurred across 5 species; five spectra from class 19 were mislabeled as class 21, and four from class 15 were misclassified as class 11. The 1-vs-world analysis had an average prediction kappa of 0.803 with a standard deviation of 3.72×10^{-2}, as indicated by the horizontal line in Figure 13.

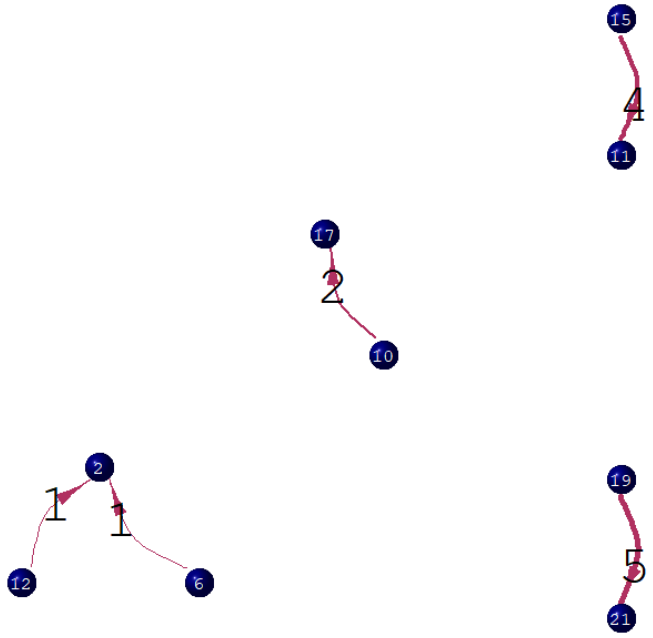

Figure 15. Network plot of flat classifier confusion matrix at the optimized delay input.

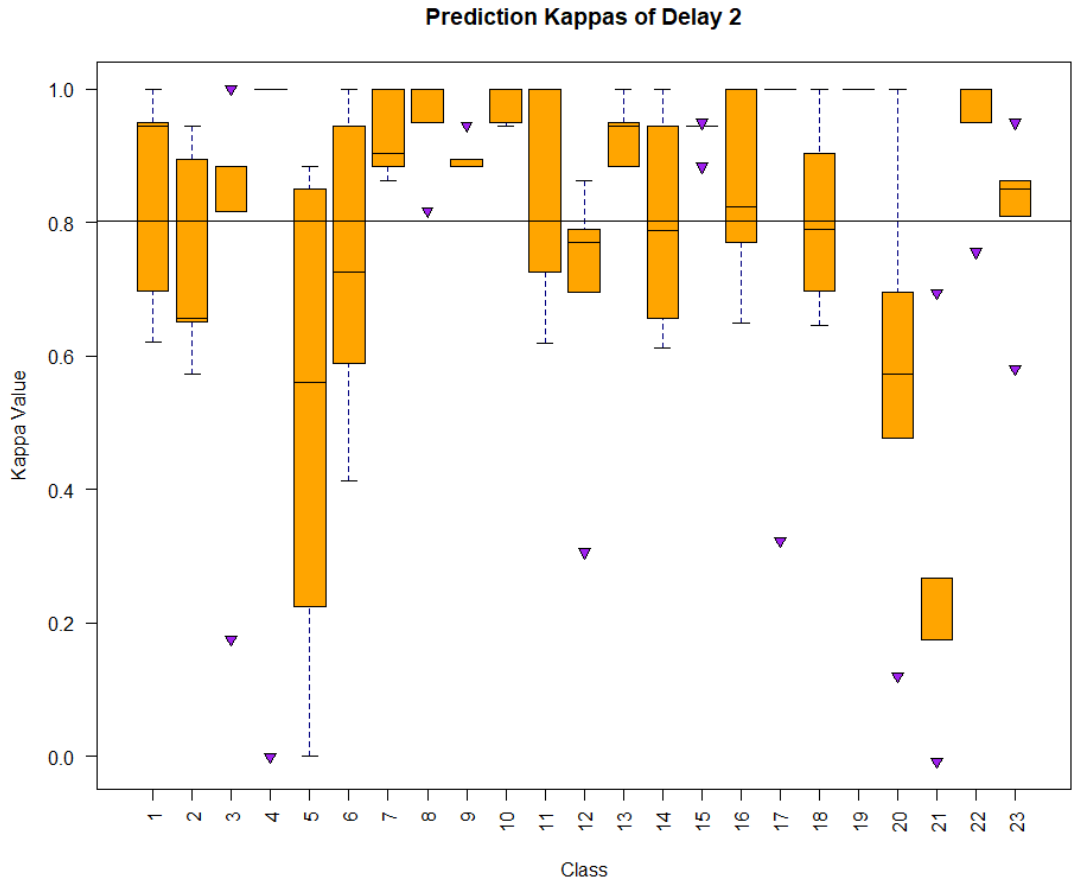

Figure 16. Boxplot of 1-vs-world classification at the optimized delay input.

Figure 15 plots the average 1-vs-world model performance of data collected at delay time 290 nanoseconds against the delay time 650 nanoseconds. Each boxplot in Fig. 12 and Fig. 14 were averaged into a singular value for each classification model. A navy-colored line of equation $y = x$ separates the plot into two equal, triangular regions. Points are plotted based on a coordinate system: the average prediction kappa value for any given class collected at 650 nanoseconds rests along the horizontal axis and, conversely, the average prediction kappa value for any given class collected at 290 nanoseconds rests along the vertical axis. A tomato-colored point indicates a 1-vs-

world classification with the respective class value at its center, while the single sea-green point indicates the flat classification performed at both delay inputs.

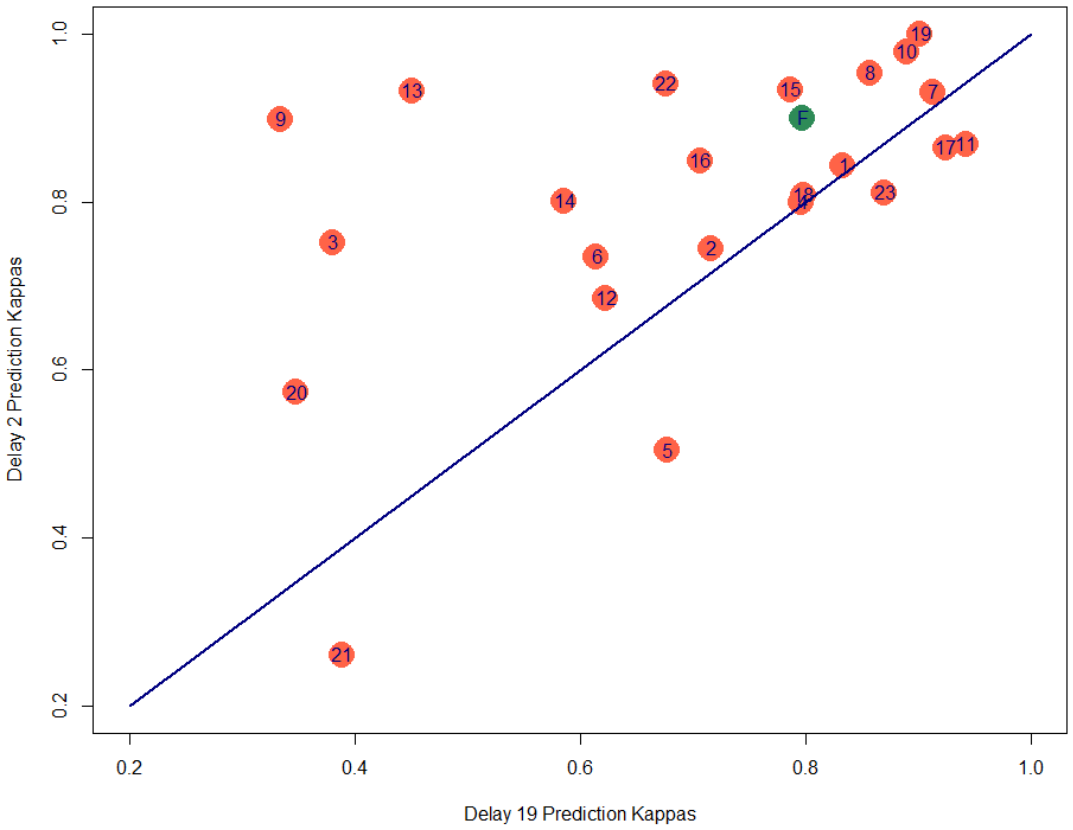

Figure 17. Scatterplot of optimized delay data against standard delay data.

Chapter 4

DISCUSSION

4.1 Optimizing Delay Input of a LIBS Handheld Analyzer

The rough optimization indicates that the optimized delay time for the given exotic hardwoods is in the range of 250 to 370 nanoseconds: an integer input ranging from 0 to 6 for the instrument. The SVM model, indicates that the optimized input is at 250 nanoseconds, while PLS indicates a maximum kappa output at 370 nanoseconds. In this range is the true value for the most robust analysis of the given hardwoods. Regression lines were plotted over both the PLS and SVM output to clearly visualize the negative linear trend associated with increasing delay input time.

The fine optimization, however, did not indicate that the optimized value for the given hardwoods is between 250 and 370 nanoseconds. Both the PLS and SVM model followed separate trends, one indicating that the factory delay setting is the ideal input value for the samples, whereas another indicated any value from 290 to the factory delay value is best for the experiment's samples of wood. Regression lines were plotted over both model output to visualize that there was a subtle, yet positive, linear trend associated with increasing delay input time.

The fine optimization failed to further prove the initial optimizations findings, that the optimized delay input is contained in the range of 250 to 370 nanoseconds. This is likely because the species of wood used in the analysis contain chemical information too similar to one another. In other woods, the species were easier to

classify relative to one another; this seems plausible given that the kappa outputs across both models in the second optimization are all within a few hundredths of a point away from a perfect kappa metric – a value of one.

4.2 Standard Delay Compared to Optimized Delay Setting

This subsequent analysis showed that, under the same preprocessing and modeling conditions, the full set of hardwoods collected at the chosen, optimized input led to a more robust classification by over a margin of 0.1, in terms of kappa. The variance among the optimized data's kappa was found to be larger than that of the standard delay's data; this is likely because there is less spectral variance across scans on the same sample and wood chips of the same species at greater delay times.

For data collected using the standard delay input, five classes that contained 8 or less samples performed poorly in a 1-vs-world classification. The models themselves were only made with 7 or less samples since a single wood chip was removed for the prediction set. Furthermore, the cross-validation implemented to assist in building the model pulled a single wood chip out for every jackknife. 3 to 6 wood samples are not nearly enough to create a robust model, especially in comparison to other species that had models constructed using upwards of 18 chips. How poorly these specific models performed is very likely a direct result of the number of wood chips available.

Similarly, data collected using the optimized delay input resulted in three species that performed poorly in a 1-vs-world classification. Two of these species are

mutual with the five aforementioned classes of wood; the third, however, is the species with the lowest quantity of samples of any given class of wood. This further indicates that the optimized delay time collects more meaningful chemical information across each sample, resolving intra-class issues that arise as a result of a smaller population of wood samples; however, there are some species – the two mutual classes – that necessitate a greater population of wood samples to properly distinguish them from other classes in a 1-vs-world analysis, regardless of what delay input at which the spectra have been collected.

As for the network plots, visualizing the misclassifications to arise from both the optimized and standardized flat classifications exemplifies that there was a significant decrease in failed predictions when decreasing the delay input time from 650 to 290 nanoseconds. There were both less species being misclassified at 290 nanoseconds, as well as less overall misclassifications – 13 compared to 105, to be precise.

Interestingly, there was a single, mutual misclassification at both delay times: 19 was, for both times, heavily misclassified as class 21. Classes 19 and 21 are *Swartzia tomentosa* and unknown, respectively. *Swartzia* originates from Latin America and class 21 has origins across the world map, located in Laos. The connection between the two isn't immediately clear given the opposite geographical origin and unknown specie name of class 21, but is worth mentioning nonetheless, especially given that collecting at different delay times appears to have little impact on how often these woods misclassify.

The last plot, Figure 15, encapsulates how the optimized delay input performs relative to the standard input. Ideally, more points would rest in the upper half of the plot than in the right half, which is the case. This indicates that any specie of wood typically better separates from all other classes and, subsequently, outputs a higher kappa metric at a delay of 290 nanoseconds than at 650.

4.3 Future Directions

Future directions include collaborations with Erin McClure-Price and Kierra Cano at the United States Department of Agriculture (USDA) to further validate the optimized delay setting and evaluate cross-handheld performance. The laboratory's Z-300 model handheld, as well as two Z-901 models, have been used to collect 5 replicate measurements at the optimized delay on 478 samples of *Dalbergia* and *Dalbergia* lookalikes spanning 18 classes at USDA Forest Service Wood Identification and Screening Center (WISC) in Ashland, Oregon.

In addition, USFS hopes to utilize handheld LIBS spectroscopy to assess a variety of domestic oakwood samples.

REFERENCES

Borduchi, L. C. L., Milori, D. M. B. P., & Villas-Boas, P. R. (2022). Study of the effects of detection times in laser-induced breakdown spectroscopy and missed variation of plasma parameters with gate width. Spectrochimica Acta Part B: Atomic Spectroscopy, 191, 106409. https://doi.org/10.1016/j.sab.2022.106409

Breinig, L., Leonhart, R., Broman, O., Manuel, A., Brüchert, F., & Becker, G. (2015). Classification of wood surfaces according to visual appearance by multivariate analysis of wood feature data. *Journal of Wood Science*, *61*(2), 89–112. https://doi.org/10.1007/s10086-014-1410-6

Celani, C. P., Lancaster, C. A., Jordan, J. A., Espinoza, E. O., & Booksh, K. S. (2019). Assessing utility of handheld laser induced breakdown spectroscopy as a means of: Dalbergia speciation. *Analyst*, *144*(17), 5117–5126. https://doi.org/10.1039/c9an00984a

Celani, C. P., McCormick, R. A., Speed, A. M., Johnston, W., Jordan, J. A., Coplen, T. B., & Booksh, K. S. (2023). Evaluation of spectral collection strategies for identification of Dalbergia spp. using handheld laser-induced breakdown spectroscopy. *Journal of Chemometrics*. https://doi.org/10.1002/cem.3479

CITES Dalbergia Checklist. (2022). Royal Botanic Gardens, Kew. file:///C:/Users/wcc93/Dropbox/CITES%20Dalbergia%20Checklist%202022%20(EN)%20(PDF).pdf

Combatting Corruption in the Timber Trade. (n.d.). Retrieved May 5, 2024, from https://www.whistleblowers.org/combatting-corruption-in-the-timber-trade/

Eilers, P. H. C. (2003). A perfect smoother. In Analytical Chemistry (Vol. 75, Issue 14, pp. 3631–3636). https://doi.org/10.1021/ac034173t

Fellin, M., Negri, M., & Zanuttini, R. (2014). Multi-elemental analysis of wood waste using energy dispersive X-ray fluorescence (ED-XRF) analyzer. *European Journal of Wood and Wood Products*, *72*(2), 199–211. https://doi.org/10.1007/s00107-013-0766-4

Gilbraith, W. E., Celani, C. P., & Booksh, K. S. (n.d.). *Visualization of Confusion Matrices with Network Graphs*.

Gruber, J., Heitz, J., Arnold, N., Ba¨uerleba¨ba¨uerle, D., Ramaseder, N., Eyer, W. M., Hocho¨rtler, J., Hocho¨rtler, H., & Koch, F. (2004). In Situ Analysis of Metal Melts in Metallurgic Vacuum Devices by Laser-Induced Breakdown Spectroscopy. In *APPLIED SPECTROSCOPY* (Vol. 58, Issue 4).

Haartveit, Y., & Flaete, O. (n.d.). *Near Infrared Spectroscopy (NIRS) as a Tool for Effective Classification of Wood*.

HH LIBS analyzer for mineral exploration. (n.d.). Retrieved March 18, 2024, from https://www.sciaps.com/post/making-a-case-for-handheld-libs-in-mineral-exploration

Illegal Logging. (n.d.). Retrieved May 5, 2024, from https://www.preferredbynature.org/sourcinghub/info/illegal-logging-0#:~:text=They%20estimate%20that%20between%2020,%2430%20and%20US%24100%20billion.

Kırbaş, İ., & Çifci, A. (2022). An effective and fast solution for classification of wood species: A deep transfer learning approach. *Ecological Informatics*, *69*, 101633. https://doi.org/10.1016/J.ECOINF.2022.101633

Lavine, B. K., Davidson, C. E., Moores, A. J., & Griffiths, P. R. (2001). Raman Spectroscopy and Genetic Algorithms for the Classification of Wood Types. *Http://Dx.Doi.Org/10.1366/0003702011953108*, *55*(8), 960–966. https://doi.org/10.1366/0003702011953108

Lednev, V. N., Dormidonov, A. E., Sdvizhenskii, P. A., Ya Grishin, M., Fedorov, A. N., Savvin, A. D., Safronova, E. S., & Pershin, S. M. (2018). Compact diode-pumped Nd:YAG laser for remote analysis of low-alloy steels by laser-induced breakdown spectroscopy. *Journal of Analytical Atomic Spectrometry*, *33*(2), 294–303. https://doi.org/10.1039/c7ja00319f

Li, W., Li, X., Li, X., Hao, Z., Lu, Y., & Zeng, X. (2020). A review of remote laser-induced breakdown spectroscopy. In *Applied Spectroscopy Reviews* (Vol. 55, Issue 1, pp. 1–25). Taylor and Francis Inc. https://doi.org/10.1080/05704928.2018.1472102

LIBS, Laser Induced Breakdown Spectroscopy, Thermo Fisher | Thermo Fisher Scientific - US. (n.d.). Retrieved March 18, 2024, from https://www.thermofisher.com/us/en/home/industrial/spectroscopy-elemental-isotope-analysis/portable-analysis-material-id/industrial-elemental-radiation-solutions/how-does-libs-work.html

McMillan, N. (n.d.). *Laser-Induced Breakdown Spectroscopy (LIBS)*. Retrieved March 18, 2024, from https://serc.carleton.edu/msu_nanotech/methods/libs.html

Park, S. Y., Kim, J. C., Kim, J. H., Yang, S. Y., Kwon, O., Yeo, H., Cho, K. C., & Choi, I. G. (2017). Possibility of wood classification in Korean softwood species using near-infrared spectroscopy based on their chemical compositions. *Journal of the Korean Wood Science and Technology*, *45*(2), 202–212. https://doi.org/10.5658/WOOD.2017.45.2.202

Qiu, Y., Wang, A., Liu, Y., Huang, D., Wu, J., Li, J., Zhang, Z., Li, X., & Wu, Q. (2020). The effect of inter-pulse delay on the spectral emission and expansion dynamics of plasma in dual-pulse fiber-optic laser-induced breakdown spectroscopy. *Physics of Plasmas*, *27*(8). https://doi.org/10.1063/5.0010570/108480

Rai, A. K., Yueh, F. Y., Singh, J. P., & Zhang, H. (2002). High temperature fiber optic laser-induced breakdown spectroscopy sensor for analysis of molten alloy constituents. *Review of Scientific Instruments*, *73*(10), 3589. https://doi.org/10.1063/1.1505101

Saeki, M., Iwanade, A., Ito, C., Wakaida, I., Thornton, B., Sakka, T., & Ohba, H. (2014). Development of a fiber-coupled laser-induced breakdown spectroscopy instrument for analysis of underwater debris in a nuclear reactor core. *Journal of Nuclear Science and Technology*, *51*(7–8), 930–938. https://doi.org/10.1080/00223131.2014.917996

Sallé, B., Cremers, D. A., Maurice, S., & Wiens, R. C. (2005). Laser-induced breakdown spectroscopy for space exploration applications: Influence of the ambient pressure on the calibration curves prepared from soil and clay samples. *Spectrochimica Acta - Part B Atomic Spectroscopy*, *60*(4), 479–490. https://doi.org/10.1016/j.sab.2005.02.009

STEINERT LSS® | LIBS – Efficient Light Metal Sorting • STEINERT. (n.d.). Retrieved March 18, 2024, from https://steinertglobal.com/us/magnets-sensor-sorting-units/sensor-sorting/libs-sorting-system/

What is LIBS? (n.d.). Retrieved March 18, 2024, from https://appliedspectra.com/technology/libs.html

Wiens, R. C., Sharma, S. K., Thompson, J., Misra, A., & Lucey, P. G. (2005). Joint analyses by laser-induced breakdown spectroscopy (LIBS) and Raman spectroscopy at stand-off distances. *Spectrochimica Acta - Part A: Molecular and Biomolecular Spectroscopy*, *61*(10), 2324–2334. https://doi.org/10.1016/j.saa.2005.02.031

Appendix A

X-RAY FLUORESCENCE SPECTROSCOPY

X-ray fluorescence (XRF) spectroscopy is a non-destructive spectroscopic technique that employs electromagnetic waves in the range of 0.01 to 10 nanometers. A Sci-aps handheld XRF Z-200 analyzer was employed for the hardwood classification. This instrument utilizes a 6 to 50 kV gold excitation source for empirical analyses alongside a 20-millimeter silicon drift detector (SDD). Much like a handheld LIBS analyzer, an Android user-interface is used for software management, archiving spectra, and device features.

A Sci-aps Z-200 XRF handheld spectrometer.

For the hardwood classification, the data acquisition was much simpler than the LIBS optimization. All 278 hardwood samples were measured 5 times at a 15 kV energy source with an integration period of 5 minutes. At energy sources greater than 15 kV, the spectra contain no chemical signals. As with the integration period, 5 minutes was implemented to improve a spectrum's signal-to-noise ratio, essentially smoothing the spectral curve.

Data manipulation followed a similar trend to the LIBS spectra. An ALS baseline correction was implemented, and a normalization algorithm was applied. After this, variable selection dependent on spectral peaks was implemented to remove signal-less regions of each scan. The pre-processed data was subsequently modeled using a linear SVM method.

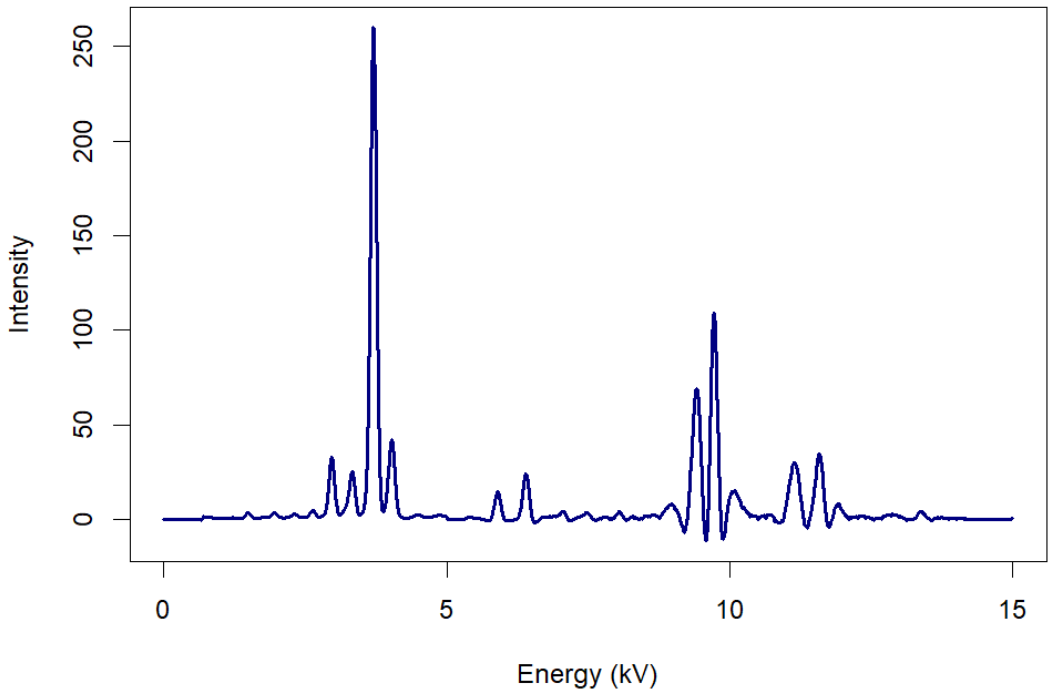

Plot of data that was collected at 15 kV. The matrix columns were baseline fit, normalized, and averaged.

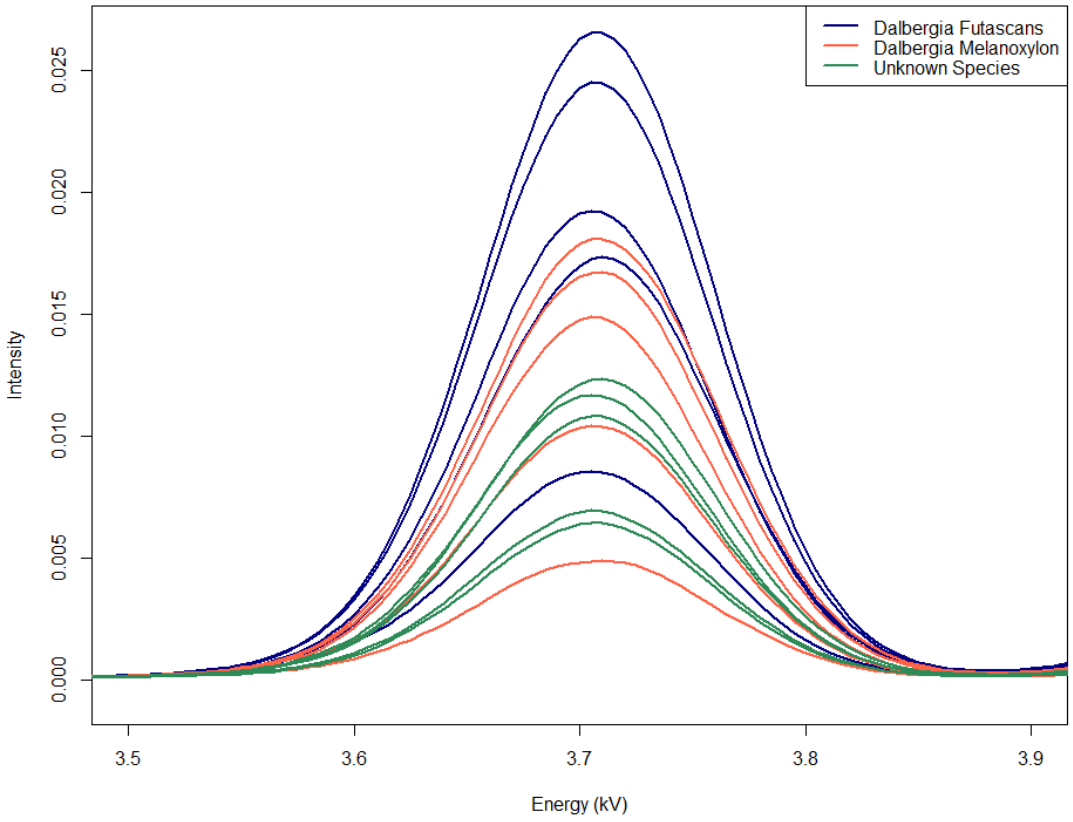

Baseline corrected, normalized spectra consisting of three species. Energy ranges from 3.5 to 3.9 kV.

The 278 wood samples were analyzed using 24 classification models: 23 1-vs-world models corresponding to each species of wood and a single flat classification. Each model was created using SVM, and the prediction kappas across five iterations were plotted as boxplots, as seen in Fig. 21. The average performance for any given boxplot is slightly under 0.2, with a large number of models performing worse than a kappa value of 0 – this indicates that simply guessing a sample's class resulted in a better accuracy metric than using the models that have been created.

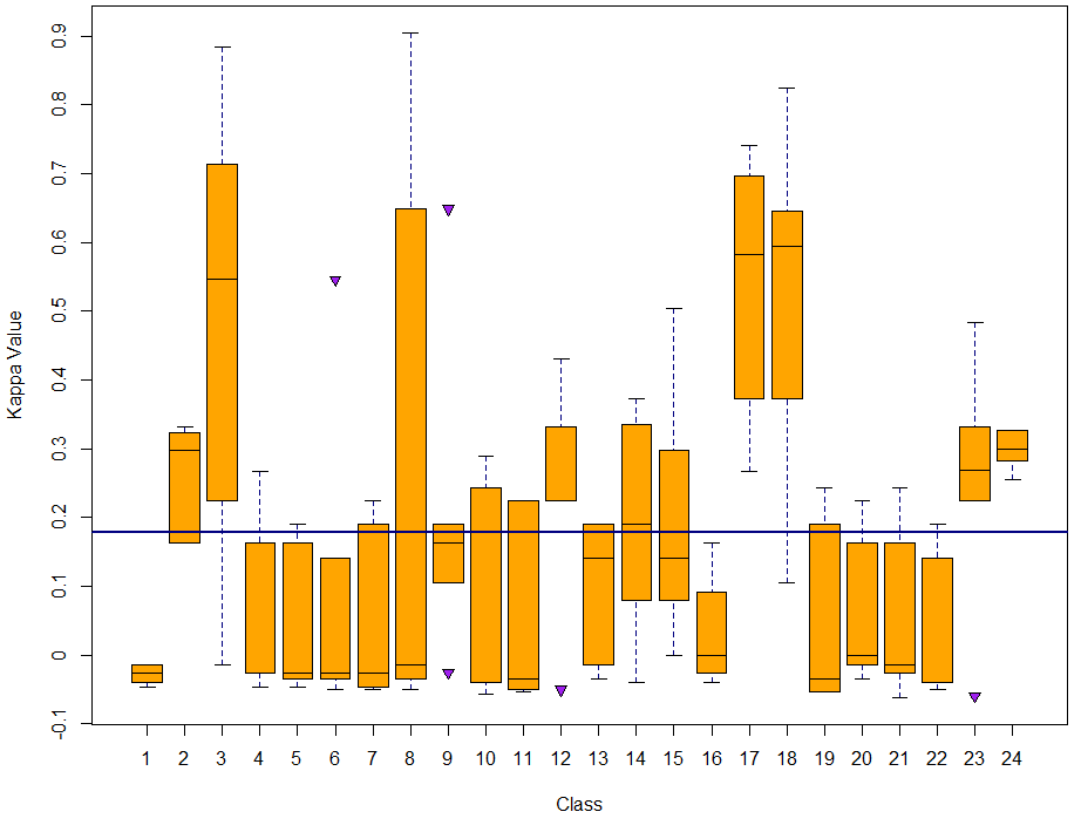

Boxplot of 1-vs-world and flat classifications at 15 kV energy source.